Applied Mathematical Modelling 125 (2024) 334–350

Contents lists available at ScienceDirect

Applied Mathematical Modelling

journal homepage: www.elsevier.com/locate/apm

A behavioural vaccination model with application to meningitis spread in Nigeria

Bruno Buonomo [a,*], Rossella Della Marca [b]

[a] Department of Mathematics and Applications, University of Naples Federico II, via Cintia, I-80126 Naples, Italy
[b] Mathematics Area, SISSA – International School for Advanced Studies, via Bonomea 265, I-34136 Trieste, Italy

ARTICLE INFO

Keywords:
Mathematical epidemiology
Meningitis
Imperfect vaccine
Information
Human behaviour

ABSTRACT

We propose a socio–epidemiological investigation of the effects of vaccine hesitancy on meningococcal meningitis transmission. The spread of the disease is described by a behavioural epidemic model. An information index is employed to take into account that the willingness to get vaccinated depends on the information and rumours about the status of the disease in the community. We show that voluntary vaccination is unable to eliminate the disease, since the control reproduction number is independent of information parameters. The model is parametrized on official data regarding the largest ever global epidemic of serogroup C meningitis occurred in Nigeria in 2016 to 2017. We reproduce both the uncontrolled phase and the controlled phase (through a vaccination campaign) of the outbreak. We estimate that the public was aware of about 69% of official data, and that the average time lag necessary for information to reach the public was 4.27 days. Our results show the potential applicability of behavioural epidemic models with information index.

1. Introduction

The meninges, membranes surrounding the brain and spinal cord, can be affected by a devastating disease, the meningitis. Although the disease affects all ages, young children are most at risk. Bacteria, fungi, viruses and parasites are the most common causes of meningitis, and the highest global burden of disease is seen with meningitis caused by bacteria. There are four main causes of acute bacterial meningitis: *Neisseria meningitidis* (meningococcus), *Streptococcus pneumoniae* (pneumococcus), *Haemophilus influenzae*, *Streptococcus agalactiae* (group B streptococcus). These bacteria were responsible for over 50% of the 250,000 deaths from all–cause meningitis in 2019 [1].

Neisseria meningitidis (Nm) is the only bacterium capable of generating large epidemics of meningococcal disease [2]. Explosive epidemics with incidence rates reaching 1,000 cases per 100,000 inhabitants have been reported, particularly in the *African meningitis belt*, an area of sub–Saharan Africa which stretches from Senegal in the west to Ethiopia in the east, involving 26 countries [1]. Nm bacteria typically live in the pharyngeal passages of healthy humans without causing symptoms. Therefore, carriers play an important role for this disease and it is believed that they represent the main source of transmission [3–5]. The bacteria, which only infect humans, are transmitted from person–to–person through respiratory droplets or throat secretions. At least 12 serotypes of meningococcus have been identified, of which groups A, B, C are responsible for about 90% of meningococcal disease cases [2].

* Corresponding author.
E-mail addresses: buonomo@unina.it (B. Buonomo), rossella.dellamarca@sissa.it (R. Della Marca).

https://doi.org/10.1016/j.apm.2023.09.031
Received 11 May 2023; Received in revised form 18 September 2023; Accepted 26 September 2023

Available online 2 October 2023

In the meningitis belt, large epidemics generally occur during the dry season between December to June, where the transmission of Nm is facilitated by overcrowded housing and mass gatherings (as pilgrimages and jamborees) [6].

According to the World Health Organization (WHO) [1], current vaccines represent the most effective way to reduce the burden and impact of meningococcal meningitis. Presently, several vaccines against Nm are available. Polysaccharide–based vaccines for serogroups A, C, W and Y, developed starting from the 1960s, are primarily used in cases of epidemic outbreaks, but they provide weak protection in infants, do not lead to herd protection as they do not prevent carriage, and generate a short–lived immune response. Therefore, they are gradually being replaced by polysaccharide–protein conjugate vaccines that are more effective in protecting infants, prevent carriage and also confer a longer–lasting immunity. As a result, this is the major class of vaccines used to prevent Nm serogroups A, C, W and Y. There are also some protein–based vaccines that are specifically designed against the serogroup B [1,7]. Recently, the MenAfriVac® vaccine against Nm serogroup A has been developed for individuals aged 9 months to 29 years [8]. Starting from 2010, MenAfriVac® has been delivered to countries in the African meningitis belt. Epidemics due to Nm serogroup A have been eliminated in vaccination areas, showing the impact of the vaccine on carriage and invasive disease, and the achievement of herd immunity [8]. Although the duration of vaccine–induced immunity is still under evaluation, the population–level immunity induced by MenAfriVac® routine vaccination is predicted to confer more than 50% protection over a period of 20 years [9,10].

Many mathematical models have been proposed to describe the transmission of bacterial meningitis [4,5,11–15]. Tuckwell et al. [15] studied a discrete–in–time epidemic model including age– and time–dependent rates of vaccination, and determined the impact of vaccination schedule on the time course of Nm serogroup C disease in France. Trotter et al. [14] developed an age–structured model that was fitted to data on Nm serogroup C conjugate vaccination in England and Wales; they investigated the direct and indirect herd immunity effects of the conjugate vaccines program. Simpson and Roberts [13] studied a Susceptible–Carriers–Ill–Recovered (SCIR) model to explore the potential effect of alternative vaccination schemes and applied the model to the case of the 2004 meningitis outbreak in New Zealand. Irving et al. [4] observed that temporary population immunity and seasonal changes in the transmissibility of infection may play an important role in meningococcal meningitis models. By using a modelling setting similar to the paper [4], Koutangni et al. [5] proposed three epidemic models to investigate the seasonal hyperendemicity for both meningococcal and pneumococcal meningitis across the meningitis belt; the models were fitted on surveillance data from Burkina Faso. Asamoah et al. [16] proposed a mathematical model for bacterial meningitis including a non–linear recovery rate that accounts for limited–resource settings; it has been shown that such non–linearity may produce the phenomenon of backward bifurcation.

In the recent years, there has been an increasing interest in investigating the degree of protection conferred by meningococcal vaccines and its implications on the disease dynamics. Djatcha Yaleu et al. [12] formulated an SCIR model for the transmission of Nm serogroup A, by assuming that the vaccine is *imperfect*, i.e. it confers only partial and temporary protection. They observed that the control of the disease can be achieved only with both large vaccination coverage and high level of vaccine efficacy. Similarly, Agusto and Leite [11] considered an SCIR model of meningococcal meningitis transmission with vaccination and studied the effect of an imperfect vaccine; the model was parametrized on the 2016/2017 epidemic of Nm serogroup C in Nigeria and the impact of the use of facial masks and vaccination was investigated through an optimal control problem.

In all the above–mentioned studies, the individuals' responses to the perceived risks associated with the status of the disease in the community are not considered. However, information and rumours about the spread of the disease may be a critical factor as to whether or not the individuals adopt protective measures, like social distancing, wearing masks, vaccination, and so on [17,18]. The case of meningitis vaccination is no exception and vaccine hesitancy represents a potential threat to the achievements of immunization programs [8,19]. In order to address this challenging issue, health policy makers periodically plan specific interventions to promote immunization against vaccine–preventable diseases like meningococcal meningitis [20].

Buonomo et al. [21] have been the first to adopt an approach based on using a distributed delay, called *information index*, to include the information–dependent vaccination in a meningococcal meningitis model. Indeed, the information index summarizes the information available on current and past disease trend [18,22]. Through such *behavioural* meningitis model the authors showed that the human behaviour may induce recurrent epidemics under certain conditions.

In this manuscript, we aim to make a further contribution to the understanding of behavioural modelling of meningococcal meningitis. For this purpose, we introduce a new SCIR model with information–dependent vaccination rate and provide an application to a real world scenario. More precisely, the model includes an imperfect vaccine and the choice of individuals to get vaccinated is assumed to be partially determined on a voluntary basis and to depend on a specific information index. We first perform a qualitative analysis based on stability and bifurcation theories and then parametrize the model using official data regarding the largest ever global epidemic of serogroup C meningitis occurred in Nigeria from December 2016 to June 2017 [23]. Numerical investigations are performed to test the ability of the model to reproduce the time evolution of the epidemic in Nigeria. Finally, the model is used to estimate the unreported data and to simulate the outcome produced by hypothetical strategies of containment enacted by health authorities.

As far as we know, this is the first time that imperfect vaccine and information–dependent vaccination rate are both incorporated into a model of meningococcal meningitis transmission. Moreover, so far the case of COVID–19 first epidemic wave in Italy is the only application of behavioural models with information index employing official data [24]. Therefore, this study provides a new example of the potential applicability of such kind of models.

The manuscript is organised as follows. In Section 2, we introduce the model by deriving the balance equations, and give some basic properties. In Section 3, we determine the basic reproduction number $\mathcal{R}_0$ and the control reproduction number $\mathcal{R}_V$; we also investigate the properties of the equilibria. A centre manifold analysis is performed in Section 4 to obtain sufficient conditions for backward or forward bifurcation at $\mathcal{R}_V = 1$. The choice of the parameters values, the simulation time frame and the initial conditions

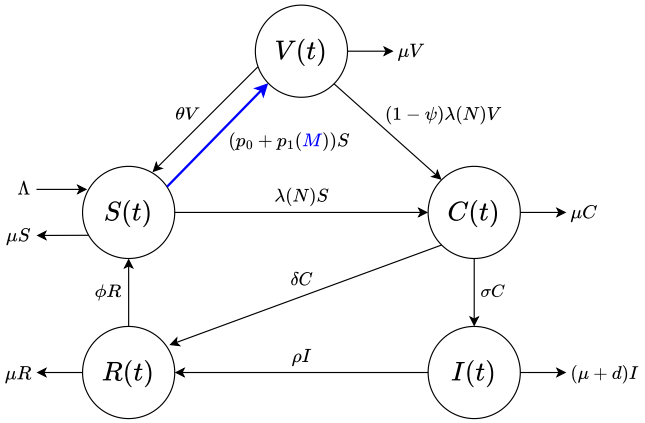

Fig. 1. Flow chart for the meningococcal meningitis model (6). The population $N(t)$ is divided into five disjoint compartments of individuals: susceptible individuals $S(t)$, vaccinated $V(t)$, carriers $C(t)$, ill individuals $I(t)$, and recovered $R(t)$. Blue colour indicates the information–dependent process in the model, where $M(t)$ is the information index (3).

of the model are described and justified in Section 5. In Section 6, we propose numerical simulations to reproduce the time evolution of the 2016/2017 Nigerian meningitis outbreak. The model is also used to simulate hypothetical scenarios. Concluding remarks are given in Section 7.

2. The model and its basic properties

We introduce a compartmental epidemic model to describe the spread of meningococcal meningitis within a population, assuming that a vaccine is available but vaccination can be not mandatory. We assume that the total population is divided into five disjoint compartments: susceptible individuals (healthy subjects who can contract the disease); vaccinated (healthy individuals that received partial and temporal protection by immunization); carriers (infected and infectious individuals that carry the Nm, but do not show signs of the invasive disease); ill individuals (infected and infectious subjects showing signs of the invasive disease); recovered (individuals who recovered after the infectious period). The time–dependent function representing the size of the aforementioned five compartments is denoted, respectively, by S, V, C, I, R. The size of the total population is denoted by N (therefore $N = S + V + C + I + R$).

The sizes of the compartments are state variables of a mathematical model, where the rate of change of each state variable is ruled by a balance equation. In the following, we describe into details all the balance equations built according to the processes illustrated in the flow chart in Fig. 1.

The model takes into account the demographic turnover given by immigration and newborns (represented by a constant net inflow Λ into the susceptible compartment), and by the natural mortality of individuals (represented by a rate μ). Disease–induced mortality of ill individuals occurs at a rate d.

The susceptible population S decreases following infection and vaccination, but vaccinated and recovered individuals become susceptible again because of the waning of vaccine–induced immunity and post–recovery immunity, respectively. The transmission is characterized by a *force of infection*, i.e. the per capita rate at which susceptible individuals become infected. Following Agusto and Leite [11], the force of infection is given by:

$$\text{FoI} = \beta \frac{\varepsilon C + I}{N}, \tag{1}$$

where β is the disease transmission rate and ε is a transmission modification factor for carriers, $\varepsilon \geq 1$. This last parameter is motivated by the asymptomatic nature of carriers, who can move freely within the population, while ill individuals are subject to identification and hospitalization.

The vaccination rate is modelled according to some important aspects of vaccine acceptance. Firstly, it is reasonable to assume that part of the population is strongly pro–vaccine or the vaccine is strongly recommended (or even mandatory) for them like in the case of high risk categories [1,6]. Such individuals are inclined to be vaccinated independently of the information. This propensity is represented by a positive constant vaccination rate p_0. Secondly, we assume that another fraction of susceptibles choose to get vaccinated because of the social alarm caused by the disease. To describe this phenomenon, we follow an approach of the *behavioural epidemiology of infectious diseases* based on the introduction of the so–called *information index* M, which summarizes the information about the current and past values of the disease [18,22]. Precisely, the vaccination rate includes also a continuous, differentiable and increasing function $p_1(M)$, such that $p_1(0) = 0$.

In the absence of empirical data about vaccinating attitudes, it is common to assume that $p_1(M)$ is a Holling type II function [25,26]:

$$p_1(M) = \left(p_{\max} - p_0\right) \frac{DM}{1 + DM}, \tag{2}$$

where $D \geq 0$ and $p_{\max} \geq p_0$. This formulation implies that $p_{\max}$ is the asymptotic overall rate when the level of circulating information is very high (say, $M \to \infty$), i.e. when there is a very high perceived risk of contagion. Moreover, the parameter D may be interpreted as a measure of how quickly the individuals react to information and voluntarily get vaccinated.

Individuals move from the susceptible compartment S to the vaccinated compartment V after vaccination. The size of the compartment V decreases due to infection, although at a reduced transmission rate $(1-\psi)\beta$, where $\psi \in (0,1]$ represents the vaccine effectiveness, and decreases also because of the waning of the vaccine–induced immunity, described by a rate θ.

Carrier individuals arise as the results of new infections of susceptible and vaccinated individuals. The carrier population C decreases at a rate σ due to transfer to the ill stage at the onset of signs of the invasive disease, and also decreases at a rate δ due to recovery.

Individuals move from the carrier compartment C to the ill compartment I after disease progression. The size of the compartment I decreases at a rate ρ because of recovery. After the infectious period, individuals from the compartments C and I move to the recovered compartment R, but as mentioned above their immunity is not permanent and become susceptible again at a rate ϕ.

The information index appearing in (2) is given by the following distributed delay:

$$M(t) = \int_{-\infty}^{t} k \frac{I(\tau)}{\bar{N}} H(\tau) a e^{-a(t-\tau)} d\tau, \tag{3}$$

where H denotes the Heaviside step function. The main assumptions behind this formulation are that the individuals react in response to the current and the past perceived risks associated to the disease, and that the memory of the population is exponentially fading. Here, as *past* we mean the period from a given initial time, say $t = 0$, to the current time. In (3), the term

$$g(t) = k \frac{I(t)}{\bar{N}}, \tag{4}$$

describes the perceived risks associated to the disease, which are assumed to depend on the size of the compartment I. The quantity $\bar{N} = \Lambda/\mu$ is a reference value (as we will see in Section 3, $\bar{N}$ is the steady state value of the total population in the disease–free case or when $d = 0$). The parameter k is the *information coverage*, which summarises two opposite phenomena in the dissemination of information: the under– and over–reporting. The under–reporting is due to technical difficulties (e.g. limited resources for case finding) or errors in data recording, and leads to underestimate the number of ill cases in the community. The over–reporting is due to media and rumours that tend to amplify the public alarm about the disease. We assume here that the former phenomenon prevails on the latter, that is $k \in (0,1]$ [27]. Finally, the quantity a in (3) is the rate parameter of the exponentially fading memory. Its inverse is the characteristic memory length and may be somehow interpreted as the average time delay in the collection of the information on the disease [18].

From (3), by applying the linear chain trick [28], we obtain the differential equation ruling the dynamics of M:

$$\dot{M} = a\left(k\frac{I}{\bar{N}} - M\right), \tag{5}$$

where the upper dot denotes the time derivative.

According to the aforementioned description, we obtain the following system of nonlinear ordinary differential equations:

$$\dot{S} = \Lambda - \beta S \frac{\varepsilon C + I}{N} - \left(p_0 + (p_{\max} - p_0)\frac{DM}{1+DM}\right) S + \theta V + \phi R - \mu S, \tag{6a}$$

$$\dot{V} = \left(p_0 + (p_{\max} - p_0)\frac{DM}{1+DM}\right) S - (1-\psi)\beta V \frac{\varepsilon C + I}{N} - (\theta + \mu) V, \tag{6b}$$

$$\dot{C} = \beta (S + (1-\psi)V) \frac{\varepsilon C + I}{N} - (\sigma + \delta + \mu) C, \tag{6c}$$

$$\dot{I} = \sigma C - (\rho + \mu + d) I, \tag{6d}$$

$$\dot{R} = \delta C + \rho I - (\phi + \mu) R, \tag{6e}$$

$$\dot{M} = a(hI - M), \tag{6f}$$

where $h = k/\bar{N} = k\mu/\Lambda$. The description of each parameter together with their baseline values is given in Table 1 in Section 6.

The initial conditions associated with model (6) are:

$$\begin{aligned} &S(0) = S_0 > 0,\ V(0) = V_0 \geq 0,\ C(0) = C_0 \geq 0, \\ &I(0) = I_0 \geq 0,\ R(0) = R_0 \geq 0,\ M(0) = M_0 \geq 0. \end{aligned} \tag{7}$$

The following proposition ensures that the solutions of model (6) are epidemiologically well–posed.

Proposition 1. *The region*

$$\Omega = \left\{ (S,V,C,I,R,M) \in \mathrm{R}^6_+ \;\middle|\; S > 0,\ S + V + C + I + R \leq \frac{\Lambda}{\mu},\ M \leq k \right\},$$

is positively invariant for model (6) with initial conditions (7).

Table 1
Temporal horizon, initial conditions and parameters values for model (6).

Parameter	Description	Baseline value	Source
t_f	Temporal horizon	27 weeks	[23]
$\bar{N}$	Total population at DFE	186,121,000	[33]
V_0	Initial number of vaccinated individuals	0	[23]
C_0	Initial number of carriers	$10I_0$	Assumed
I_0	Initial number of ill individuals	14	[23]
R_0	Initial number of recovered individuals	0	Assumed
M_0	Initial value of the information index	$kI_0/\bar{N}$	Assumed
$\mathcal{R}_0$	Basic reproduction number	1.889	See (9)
μ	Natural mortality rate	$1/54$ years^{-1}	[34]
β	Transmission rate	0.27 days^{-1}	See Section 5
ε	Modification factor w.r.t. transmission from C	1	[11]
p_0	Information–independent vaccination rate	$0 - 0.01p_{\max}$	Assumed
$p_{\max}$	Upper bound of overall vaccination rate	0.01 days^{-1}	Estimated from [25,35–37]
D	Reactivity factor to voluntary vaccination	$0 - 6.5 \cdot 10^3$	See Section 5
ψ	Vaccine effectiveness	0.85	[11,38]
θ	Waning rate of vaccine–induced immunity	$1/5$ years^{-1}	[11,38]
σ	Rate at which carriers develop symptoms	0.0051 years^{-1}	See Section 5
δ	Recovery rate for carriers	$1/7$ days^{-1}	Estimated from [5]
ρ	Recovery rate for ill individuals	0.1128 days^{-1}	[11]
d	Disease–induced mortality rate	0.01 days^{-1}	See (20)
ϕ	Waning rate of natural immunity	0.0032 days^{-1}	[11]
k	Information coverage	0.6945	See Section 5
a	Inverse of information delay	0.2341 days^{-1}	See Section 5

Proof. See Appendix A.1. □

3. Equilibria and their properties

Let us begin by looking for equilibria of model (6) such that $C = I = 0$. The only *disease–free equilibrium* (DFE) is given by

$$\text{DFE} = \left(\bar{S}, \bar{V}, 0, 0, 0, 0\right) = \left(\frac{\Lambda(\theta+\mu)}{\mu(p_0+\theta+\mu)}, \frac{\Lambda p_0}{\mu(p_0+\theta+\mu)}, 0, 0, 0, 0\right). \tag{8}$$

Note that $\bar{S} + \bar{V} = \bar{N}$.

In the next proposition two important quantities are derived in terms of the parameters of the system. The first quantity is the well–known *basic reproduction number*, $\mathcal{R}_0$, which is frequently used as an indicator for measuring the potential spread of an infectious disease within a community. The second quantity is the *control reproduction number*, $\mathcal{R}_V$, which has the same meaning of $\mathcal{R}_0$ but refers to the controlled phase of the epidemic when a vaccination campaign is implemented and therefore depends on the vaccination–related parameters p_0, ψ, θ.

Proposition 2. *The basic reproduction number of model (6) is given by*

$$\mathcal{R}_0 = \beta \frac{\varepsilon(\rho+\mu+d)+\sigma}{(\sigma+\delta+\mu)(\rho+\mu+d)}, \tag{9}$$

and the control reproduction number is given by

$$\mathcal{R}_V = \mathcal{R}_0 \frac{(1-\psi)p_0+\theta+\mu}{p_0+\theta+\mu}. \tag{10}$$

Proof. See Appendix A.2. □

From Proposition 2, it follows that [29]:

Proposition 3. *If $\mathcal{R}_V < 1$, then the DFE is locally asymptotically stable. If $\mathcal{R}_V > 1$, then the DFE is unstable.*

Remark 1.

i) Let us denote the fraction of the population vaccinated at DFE as

$$\bar{p} = \frac{\bar{V}}{\bar{N}} = \frac{p_0}{p_0+\theta+\mu}.$$

It follows that

$$\mathcal{R}_V = \mathcal{R}_0 (1 - \psi \bar{p}), \tag{11}$$

where the equality holds only if $p_0 = 0$ (i.e., $\bar{p} = 0$) or $\psi = 0$. That is, although being imperfect, the vaccine (characterized by $p_0 > 0$ and $0 < \psi \leq 1$) reduces the reproduction number of the disease.

ii) It is possible to determine a threshold for the fraction $\bar{p}$, below which small perturbations of the DFE may lead to epidemic outbreaks. Infact, from $\mathcal{R}_V > 1$ it follows $\bar{p} < p_c$, where $p_c = \left(1 - 1/\mathcal{R}_0\right)/\psi$.

Proposition 4. *If $\mathcal{R}_0 \leq 1$, then the DFE is globally asymptotically stable.*

Proof. See Appendix A.3. □

Now, we determine the existence of *endemic* equilibria (EE) of model (6), i.e. equilibria such that $C \neq 0$ and $I \neq 0$. Let us denote by $\mathrm{EE} = (S_e, V_e, C_e, I_e, R_e, M_e)$ the generic endemic equilibrium and, for convenience, introduce the quantities:

$$q_1 = \theta + \mu, \;\; q_2 = \sigma + \delta + \mu, \;\; q_3 = \rho + \mu + d, \;\; q_4 = \phi + \mu. \tag{12}$$

From model (6), the components of EE can be written as functions of $\lambda_e = \beta(\varepsilon C_e + I_e)/N_e$ (see (1)), where N_e is the size of the total population at the endemic equilibrium, i.e. $N_e = (\Lambda - d I_e)/\mu$, see (22). One gets:

$$\begin{aligned}
S_e &= \frac{(1-\psi)\lambda_e + q_1}{(1-\psi)(\lambda_e + p_e) + q_1} \frac{\Lambda q_2 q_3}{\beta\mu(\varepsilon q_3 + \sigma) + \sigma d \lambda_e}, \\
V_e &= \frac{p_e}{(1-\psi)(\lambda_e + p_e) + q_1} \frac{\Lambda q_2 q_3}{\beta\mu(\varepsilon q_3 + \sigma) + \sigma d \lambda_e}, \\
C_e &= \frac{\Lambda q_3 \lambda_e}{\beta\mu(\varepsilon q_3 + \sigma) + \sigma d \lambda_e}, \\
I_e &= \frac{\Lambda \sigma \lambda_e}{\beta\mu(\varepsilon q_3 + \sigma) + \sigma d \lambda_e}, \\
R_e &= \frac{\Lambda(\delta q_3 + \sigma\rho)\lambda_e}{q_4(\beta\mu(\varepsilon q_3 + \sigma) + \sigma d \lambda_e)}, \\
M_e &= \frac{h\Lambda\sigma\lambda_e}{\beta\mu(\varepsilon q_3 + \sigma) + \sigma d \lambda_e},
\end{aligned} \tag{13}$$

where $p_e = p_0 + p_1(M_e)$, see (2).

By substituting the expressions (13) in the right–hand side of the equation (6a), one obtains the third degree polynomial

$$b_3 \lambda_e^3 + b_2 \lambda_e^2 + b_1 \lambda_e + b_0, \tag{14}$$

where

$$b_0 = (p_0 + q_1) q_2 q_3 q_4 \Lambda^2 \sigma^2 \mu (1 - \mathcal{R}_V),$$

and b_3, b_2, b_1 are quantities containing numerous terms, each of them depending on the model parameters. Since we do not need the exact expressions of b_3, b_2, b_1 for developing our analysis, we do not report them for the sake of simplicity. However, it could be seen that the quantity b_3 is strictly positive. Later, in Section 6, we will numerically compute the roots of the polynomial (14) in the case of the 2016/17 Nigerian meningitis outbreak.

It is sufficient to use the Descartes' rule of signs to state the following result:

Proposition 5. *If $\mathcal{R}_V < 1$, then model (6) admits either zero or two endemic equilibria. If $\mathcal{R}_V > 1$, then model (6) admits either one or three endemic equilibria.*

Remark 2. One can easily verify that, in absence of vaccination ($p_0 + p_1(M) = 0$ in model (6) and therefore $\mathcal{R}_V = \mathcal{R}_0$), there are no endemic equilibria if $\mathcal{R}_0 < 1$ and there is an unique endemic equilibrium if $\mathcal{R}_0 > 1$. This is in agreement with the results obtained by Agusto and Leite *[11]*.

4. Centre manifold analysis

Since it is difficult to obtain analytical insights regarding the stability of endemic equilibria of model (6), we use a bifurcation theory approach to investigate this issue for values of the control reproduction number $\mathcal{R}_V$ close to the critical value $\mathcal{R}_V = 1$. A nowadays classical result is that, under general conditions usually satisfied by epidemic models, the local stability of a non–hyperbolic equilibrium may be obtained by studying the equation [29–31]:

$$\dot{u} = A u^2 + B \beta u, \tag{15}$$

where

$$A = \frac{v}{2} \cdot D_{xx} f(\mathrm{DFE}, \beta_c) w^2 \equiv \frac{1}{2} \sum_{k,i,j=1}^{6} v_k w_i w_j \frac{\partial^2 f_k(\mathrm{DFE}, \beta_c)}{\partial x_i \partial x_j}, \tag{16}$$

and

$$B = v \cdot D_{x\beta} f(\mathrm{DFE}, \beta_c) w \equiv \sum_{k,i=1}^{6} v_k w_i \frac{\partial^2 f_k(\mathrm{DFE}, \beta_c)}{\partial x_i \partial \beta}. \tag{17}$$

Equation (15) is the normal form representing the dynamics of the system on the centre manifold [32]. In (16) and (17) the parameter β is the bifurcation parameter, β_c is the critical value of β, $x = (S, V, C, I, R, M)$ is the state variables vector, f is the right–hand side of system (6), and v and w denote, respectively, the left and right eigenvectors corresponding to the null eigenvalue of the Jacobian matrix evaluated at criticality (i.e. at DFE and $\beta = \beta_c$).

Observe that $\mathcal{R}_V = 1$ is equivalent to:

$$\beta = \beta_c := \frac{(p_0 + q_1) q_2 q_3}{((1-\psi) p_0 + q_1)(\varepsilon q_3 + \sigma)},$$

where q_1, q_2, q_3 are given in (12), so that the DFE is locally asymptotically stable if $\beta < \beta_c$, and it is unstable if $\beta > \beta_c$.

The direction of the bifurcation occurring at $\beta = \beta_c$ can be derived from the sign of the coefficients (16) and (17). More precisely, if $A > 0$ (resp. $A < 0$) and $B > 0$, then at $\beta = \beta_c$ there is a backward (resp. forward) transcritical bifurcation.

In our case, the Jacobian matrix of system (6) evaluated at DFE (8) for $\beta = \beta_c$ is

$$J(\mathrm{DFE}, \beta_c) = \begin{pmatrix} -(p_0+\mu) & \theta & -\frac{\beta_c \varepsilon}{\bar{N}} \bar{S} & -\frac{\beta_c}{\bar{N}} \bar{S} & \phi & -p_1'(0) \bar{S} \\ p_0 & -q_1 & -(1-\psi) \frac{\beta_c \varepsilon}{\bar{N}} \bar{V} & -(1-\psi) \frac{\beta_c}{\bar{N}} \bar{V} & 0 & p_1'(0) \bar{S} \\ 0 & 0 & -\frac{q_2 \sigma}{\varepsilon q_3 + \sigma} & \frac{q_2 q_3}{\varepsilon q_3 + \sigma} & 0 & 0 \\ 0 & 0 & \sigma & -q_3 & 0 & 0 \\ 0 & 0 & \delta & \rho & -q_4 & 0 \\ 0 & 0 & 0 & ah & 0 & -a \end{pmatrix},$$

where $p_1'(0) = (p_{\max} - p_0) D$ (see (2)), and q_4 is given in (12). The spectrum of $J(\mathrm{DFE}, \beta_c)$ is

$$\Sigma = \left\{ 0, -(p_0 + q_1), -q_4, -\mu, -a, -\frac{q_3(\varepsilon q_3 + \sigma) + q_2 \sigma}{\varepsilon q_3 + \sigma} \right\}.$$

Therefore, when $\beta = \beta_c$ (or, equivalently, when $\mathcal{R}_V = 1$), the DFE is a non–hyperbolic equilibrium, since $J(\mathrm{DFE}, \beta_c)$ admits a simple zero eigenvalue and the other eigenvalues have negative real part. It can be easily checked that the vectors

$$\begin{aligned} v &= \left(0, 0, \frac{\varepsilon q_3 + \sigma}{q_2}, 1, 0, 0\right), \\ w &= \left(w_1, w_2, \frac{q_3}{\sigma} w_4, w_4, \frac{\delta q_3 + \sigma \rho}{\sigma q_4} w_4, h w_4\right)^T, \end{aligned} \tag{18}$$

where

$$\begin{aligned} w_1 &= \left(\frac{\phi(\delta q_3 + \sigma \rho) - q_2 q_3 q_4}{\sigma q_4 \mu} \right) w_4 - w_2, \\ w_2 &= \frac{w_4}{\sigma(p_0 + q_1)} \left(p_0 \frac{\phi(\delta q_3 + \sigma \rho) - q_2 q_3 q_4}{q_4 \mu} + \beta_c \frac{\bar{S}}{\bar{N}} \left(\varepsilon q_3 + \sigma\right) - q_2 q_3 + p_1'(0) h \sigma \bar{S} \right), \\ w_4 &= \frac{q_2 \sigma}{q_3 \left(\varepsilon q_3 + \sigma\right) + q_2 \sigma}, \end{aligned} \tag{19}$$

are left and right eigenvectors, respectively, associated with the zero eigenvalue and $v \cdot w = 1$. From (16) and (17) we get

$$\begin{aligned} A &= v_3 \left(\sum_{i=1}^{5} w_i \sum_{j=3, j \neq i}^{4} w_j \frac{\partial^2 f_3(\mathrm{DFE}, \beta_c)}{\partial x_i \partial x_j} + \sum_{i=3}^{4} \frac{w_i^2}{2} \frac{\partial^2 f_3(\mathrm{DFE}, \beta_c)}{\partial x_i^2} \right) \\ &= v_3 (\varepsilon w_3 + w_4) \frac{\beta_c}{\bar{N}^2} \left(\psi(w_1 \bar{V} - w_2 \bar{S}) - (w_3 + w_4 + w_5)(\bar{S} + (1-\psi)\bar{V}) \right), \end{aligned}$$

and

$$B = v_3 \sum_{i=3}^{4} w_i \frac{\partial^2 f_3(\mathrm{DFE}, \beta_c)}{\partial x_i \partial \beta} = v_3 (\varepsilon w_3 + w_4) \frac{\bar{S} + (1-\psi)\bar{V}}{\bar{N}},$$

where v_3, w_3, $w_4 > 0$. Then, $B > 0$ and the local dynamics of system (6) around the DFE is determined by the sign of A. We have two cases:

- if $A > 0$, then, when $\beta < \beta_c$, with $|\beta - \beta_c| \ll 1$, the DFE is locally asymptotically stable, and there exists an unstable endemic equilibrium; when $\beta > \beta_c$, with $\beta - \beta_c \ll 1$, the DFE is unstable;
- if $A < 0$, then, when $\beta - \beta_c$ changes from negative to positive, the locally asymptotically stable DFE becomes unstable, and a locally asymptotically stable endemic equilibrium emerges.

The above result may be summarized as follows.

Proposition 6. *Model (6) exhibits a forward (resp. backward) bifurcation at DFE and* $\mathcal{R}_V = 1$ *if*

$$\psi(w_1\bar{V} - w_2\bar{S}) - (w_3 + w_4 + w_5)(\bar{S} + (1-\psi)\bar{V}) < 0 \quad (resp. > 0),$$

where $\bar{S}$, $\bar{V}$ *are given in (8) and* w_i, $i = 1, \dots, 5$, *are given in (18)–(19).*

5. Parametrization

The meaning of the parameters included in model (6) and their baseline values are reported in Table 1, together with the simulation time frame and the initial conditions. The baseline values are obtained by using the official data regarding the largest ever global epidemic of serogroup C meningitis occurred in Nigeria [23]. In this section, we give a detailed account of the parametrization.

(*a*) *Initial conditions and time frame*

An unknown febrile illness started to affect several people in the Nigerian state of Zamfara at the end of November 2016, across Birnin Magaji, Maradun and Zurmi local government areas (LGAs) [39]. Initially managed as severe malaria, only in the second epidemiological week of 2017 laboratory results of cerebrospinal fluid samples taken from affected individuals resulted positive for Nm serogroup C. Once obtained confirmation of meningococcal meningitis, a retrospective re–classification of the cases was done and, consequently, Birnin Magaji crossed the alert threshold in the epidemiological week 50 of 2016 (December 12–18). The disease rapidly spread to other Nigerian states and this escalated into a full blown epidemic as a result of an exponential increase in the number of cases and deaths [39–41]. The incidence of suspected cases peaked in epidemiological weeks 14 and 15 of 2017 and showed a steady decline from the week 16. Vaccination campaigns were conducted in the most affected states starting from April 5, 2017, for a total of about 2.1 million vaccinated people. On June 23, 2017 (i.e. during epidemiological week 25), the Nigeria Federal Ministry of Health officially declared the end of the outbreak in the country, after no evidence of outbreak–linked cases for two consecutive weeks [39–41].

The Nigeria Centre for Disease Control (NCDC) reported the incidence of suspected cases and deaths on a weekly basis starting from the end of the epidemiological week 50 of 2016, during which 14 new cases and no deaths were registered [23]. A suspected case of meningitis was defined as the sudden onset of fever with body temperature higher than $38\,^{\circ}$C (i.e., $100.4\,^{\circ}$F), and at least one meningeal sign, including neck stiffness or altered consciousness in any person, or a bulging anterior fontanelle in children aged less than 18 months [40]. Hence, asymptomatic carriers were not traced.

Now, we set the initial conditions (7). As initial time $t = 0$ we consider the day when the first data by NCDC were provided and disregard previous unreported cases. Therefore, we set the starting day of the outbreak to December 18, 2016, that is the end of the epidemiological week 50. At that time, there were reported 14 suspected cases and no vaccinated and recovered people, that is $I_0 = 14$, $V_0 = 0$ and $R_0 = 0$. As for C_0, there are no official data available for carriers and the time profiles of the model solutions are sensitive to the variation of this value. We found that assuming C_0 to be in the order of ten times as the ill cases provides a good fit with official data over time. Therefore, we set $C_0 = 140$. As for the initial value of the information index, it is set to $M_0 = kI_0/\bar{N}$. This quantity represents the 'initial' perceived risk associated to the disease according to (4). Finally, the initial value of susceptible individuals is obtained from $S_0 = N(0) - V_0 - C_0 - I_0 - R_0$, where $N(0)$ is approximated to the steady state value of the total population before the outbreak, namely $N(0) = \bar{N}$ (see (8)).

The final week of the considered time frame is the epidemiological week 25 of 2017, when the outbreak was declared over [41], that is $t_f = 27$ weeks.

(*b*) *Demographic and epidemiological parameters*

According to the demographic statistic bulletin of the Nigerian National Bureau of Statistics [33], the total resident population of Nigeria in 2016 was approximately $186,121,000$ inhabitants, which we take as value for $\bar{N}$. The life expectancy at birth in the same year was estimated to be 54 years [34], so that the natural mortality rate is $\mu = 1/54$ years^{-1}, yielding $\Lambda = \mu\bar{N} \approx 9,437$ days^{-1}.

The values of the epidemiological parameters ρ and ϕ are taken from the estimates obtained by Agusto and Leite [11] in the case of constant vaccination rate and no behavioural response (that is, our model (6) with $p_1(M) = 0$, where p_1 is given in (2)). Based on the available data on the meningitis outbreak in Nigeria from the epidemiological week 5 to the week 27 of 2017, they found that the average time for recovery from invasive disease was about 9 days (corresponding to $\rho = 0.1128$ days^{-1}), and the average time duration of the disease–induced immunity was about 10 months (corresponding to $\phi = 0.0032$ days^{-1}). As done by Agusto and Leite

[11], we also assume that $\varepsilon = 1$, i.e. the disease transmission factor from carriers and from ill individuals was the same during that outbreak.

For meningococcal bacteria in general, it is not clear how long the individuals can carry the bacteria, although it is known that carriage is not permanent and generally lasts weeks to months and varies by person and with strains of the bacteria [42]. In the modelling study by Koutangni et al. [5], it has been estimated a carriage duration of approximately 1 week. Therefore, here we take the recovery rate of carriers as $\delta = 1/7$ days^{-1}.

In order to estimate the disease–induced mortality rate, we use a formula given by Day [43], which has been also used in modelling outbreaks of respiratory viruses [24,44]:

$$d = (1 - \mu\Theta)\frac{C_F}{\Theta}, \tag{20}$$

where C_F is the fatality rate and Θ is the expected time from the onset of symptoms until death. The case fatality rate of the 2016/2017 Nigerian meningitis outbreak was $C_F = 8\%$ [40,41]. We also assume $\Theta = 8$ days since the first cases of deaths were registered during the epidemiological week 52 of 2016, that is more than a week after the first suspected cases [23]. Hence, from (20) we get $d \approx 0.01$ days^{-1}.

Finally, it remains to select the values of the transmission rate β and of the rate σ at which carriers develop symptoms. To this aim, we search for the values that best fit with the 'uncontrolled' phase of the 2016/2017 meningitis outbreak in Nigeria. More precisely, since the vaccination campaign started on April 5, 2017 (i.e. epidemiological week 14) [39,41], we account for the number of suspected cases of meningitis, from the epidemiological week 50 of 2016 to the week 13 of 2017 (note that we assume that suspected cases are in fact confirmed ill cases). By setting $\beta = 0.27$ days^{-1} and $\sigma = 0.0051$ years^{-1} in model (6) with $p_0 + p_1(M) = 0$, we obtain a quite good fit with the curves of the weekly and the cumulative suspected cases (see Fig. 3).

(*c*) *Vaccination–related parameters*

Starting from April 2017, the National Primary Health Care Development Agency, responsible for vaccination activities in Nigeria, had both polysaccharide and conjugate vaccines available to mitigate the meningitis outbreak [40,41]. Because of the limited vaccine supplies, vaccine use was prioritized to the most affected LGAs in Katsina, Sokoto, Yobe, and Zamfara states. The targeted population was from 1 to 29–years old, who made up 70% of the population and 90% of the total cases [38]. In April–May 2017, approximately 2.1 million people were vaccinated, that is 84.4% of the highest risk age group in the most affected LGAs. Extensive social mobilization activities, including outreach to community leaders and engagement on social and traditional media, helped to rise awareness and to facilitate desired behavioural change, including vaccine acceptance and avoidance of overcrowding, thereby reducing potential for continued transmission [40,41].

Following [11,38], we consider that the vaccine had effectiveness of 85% and was able to confer an immunity lasting on average 5 years, that is we set $\psi = 0.85$ and $\theta = 1/5$ years^{-1}. We also assume that the upper bound $p_{\max}$ of the overall vaccination rate is $p_{\max} = 0.01$ days^{-1}. This value is in line with data concerning the 2009 H1N1 pandemic influenza, whose daily rate of vaccine administration was below 2% of the total population (see [36] and references therein). Furthermore, threshold values of 1–2% *per* day were also considered in epidemic models of dengue, cholera and COVID–19 diseases [25,35,37]. We finally assume an information–independent vaccination rate $p_0 = 0.01 p_{\max}$ during the vaccination campaign.

(*d*) *Information–related parameters*

The information–related parameters are the reactivity factor to voluntary vaccination D, the information coverage k and the inverse of the characteristic memory length a. The vaccination campaign started on April 5, 2017 (i.e., epidemiological week 14) [39,41] and the only available official data is the cumulative number of vaccinated individuals at the end of the campaign. In our simulations, the first day of the campaign corresponds to the beginning of the 16th week (before then we take $p_0 = D = 0$, so that $p_0 + p_1(M) = 0$). The initial growth of the cumulative number of vaccinated individuals is assumed to be linear, which can be obtained by setting $D = 6,500$.

In order to estimate k and a, we search for the pair (k, a) which gives:

$$(k_{\min}, a_{\min}) = \arg\min_{(k,a)} |\mathrm{CV}_o - \mathrm{CV}_m|, \tag{21}$$

where CV_o is the official number of total vaccinated individuals during the campaign, $\mathrm{CV}_o = 2.1 \cdot 10^6$ individuals, and CV_m is the same quantity as predicted by model (6), i.e.

$$\mathrm{CV}_m = \int_0^{t_f} \left(p_0 + (p_{\max} - p_0)\frac{DM(t)}{1 + DM(t)} \right) S(t)dt.$$

From the contour plot in Fig. 2 we note that the quantity $\mathrm{CV}_o - \mathrm{CV}_m$ decreases with increasing k, while it is almost unaffected by variation of a, except for $a < 0.05$ days^{-1} (that is $1/a > 20$ days), where CV_m rapidly decreases with decreasing a.

The minimum required in (21) is obtained at $(k_{\min}, a_{\min}) = (0.6945, 0.2341 \text{ days}^{-1})$. We interpret such values as follows. The level of awarenesses of the population regarding the number of ill cases (normalized with respect to $\bar{N}$) was approximately 69%. This value may be seen as a resulting from the balance between the disease under–reporting and the media and rumours amplification of the social alarm. The information took on average $1/a_{\min} \approx 4.3$ days to reach the general public. This value is consistent with the

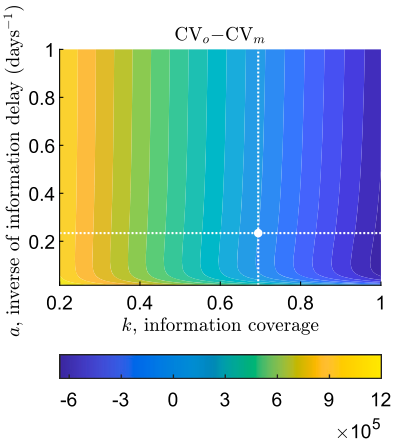

Fig. 2. Contour plot of the difference between CV_o, the official number of total vaccinated individuals during the campaign, and CV_m, the same quantity as predicted by model (6), as a function of both the information coverage k, ranging from 0.2 to 1, and the inverse of the information delay a, ranging from 1/60 days^{-1} to 1 days^{-1}. The number of discretization points for both k and a is 200. The intersection of dotted white lines indicates the corresponding baseline values. Initial conditions and parameter values are given in Table 1.

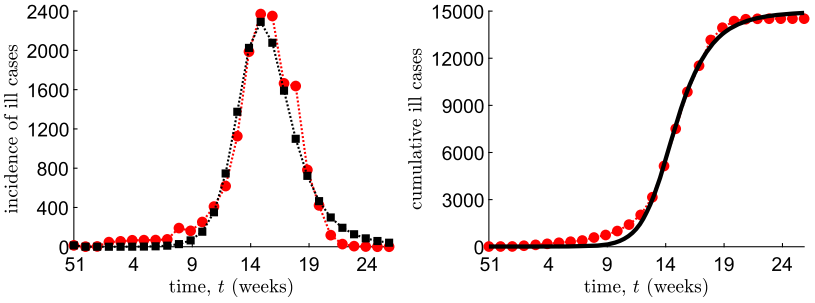

Fig. 3. Comparison between the official data of 2016/2017 Nigerian outbreak (red dots) and the solutions of model (6) (black lines). Left panel: weekly incidence of ill cases. Right panel: cumulative ill cases. The ticks on the horizontal axis correspond to the first day of the indicated epidemiological week. Initial conditions and parameter values are given in Table 1.

weekly frequency at which NCDC reports were produced [23] (which corresponds to an average time from manifestation of cases to report of approximately 4 days).

6. Modelling the 2016/2017 Nigerian meningitis outbreak

In this section, we reproduce the time evolution of the 2016/2017 Nigerian meningitis outbreak by using the SCIR model with information–dependent vaccination rate (6). Numerical simulations are performed in MATLAB [45]. We use the `ode45` solver for integrating the system and the platform–integrated functions for getting the plots.

In Fig. 3, it is shown a comparison between the official data of the Nigerian outbreak and the solutions of model (6), where we identify the ill cases with the suspected cases reported by Nigerian health authorities. The left panel refers to the incidence of ill cases at each week j, WI_j, and the right panel refers to the cumulative number of ill cases at time t, CI. According to model (6), we have

$$WI_j = \int_{7j-6}^{7j} \sigma C(t)dt, \quad CI = \int_0^t \sigma C(\tau)d\tau,$$

where j denotes the j–th week and t is measured in days.

From Fig. 3, we note that the model closely reproduces the official data. In particular, the match turns to be rather good during the acute phase of the outbreak (i.e. from epidemiological week 9 to week 19 of 2017), while the official data are slightly underestimated (resp. overestimated) at the beginning (resp. at the end) of the outbreak. This discrepancy can be explained by the fact that the effect of stochasticity could be relevant and should be taken into account when dealing with low quantities.

During the first phase of the epidemic, when vaccination was not yet available (i.e. from epidemiological week 50 of 2016 to week 13 of 2017), a total number of 5,229 ill cases is estimated versus 5,140 officially reported (+1.7%); whilst at the end of the epidemic (i.e. at the end of epidemiological week 25 of 2017) the model estimates 14,885 ill cases versus 14,518 officially reported (+2.5%).

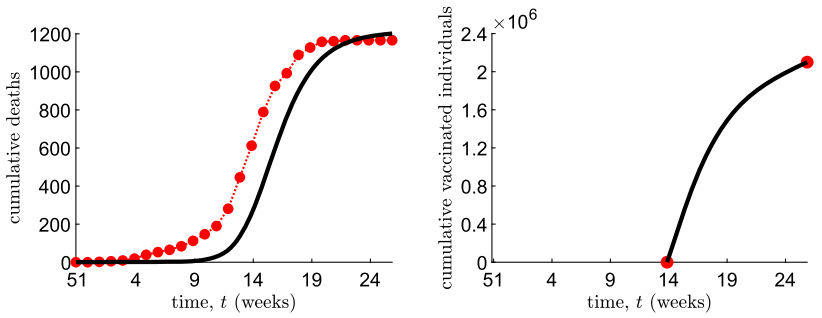

Fig. 4. Comparison between the official data of 2016/2017 Nigerian outbreak (red dots) and the solutions of model (6) (black lines). Left panel: cumulative deaths. Right panel: cumulative vaccinated individuals. The ticks on the horizontal axis correspond to the first day of the indicated epidemiological week. Initial conditions and parameter values are given in Table 1.

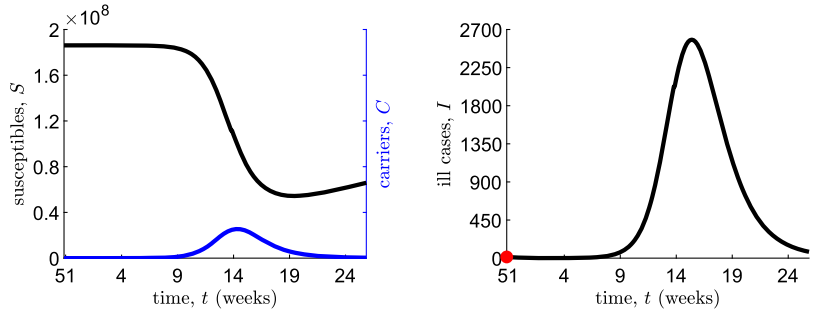

Fig. 5. Epidemic evolution predicted by model (6). Left panel: susceptibles (black line) and carriers (blue line). Right panel: ill cases. The red dot indicates the number of suspected cases registered at the beginning of the epidemic, i.e. 14 cases [23]. The ticks on the horizontal axis correspond to the first day of the indicated epidemiological week. Initial conditions and parameter values are given in Table 1.

In Fig. 4, the comparison between the official data and the numerical simulations refers to the cumulative number of deaths, CD (left panel) and the cumulative number of vaccinated individuals, CV (right panel). These quantities at time t are given by:

$$\mathrm{CD} = \int_0^t dI(\tau)d\tau, \quad \mathrm{CV} = \int_0^t \left(p_0 + (p_{\max} - p_0)\,\frac{DM(\tau)}{1+DM(\tau)}\right) S(\tau)d\tau.$$

From the left panel, it can be observed that the model is able to reproduce the data in the initial and final stages of the outbreak, while a sort of time lag, with an average of 17.5 days, can be noticed between data and numerical solutions during the intermediate stage. This delay could be due to the procedure used to collect the data. Indeed, the reports by Nigerian health authorities regarding *Survived* and *Died* individuals for each given epidemiological week were continuously updated, probably indicating that deceased individuals may have been recorded at the time of onset of the disease and not at the time of their death. This kind of recording could justify the observed delay in the time series of cumulative deaths produced by model (6). In any case, the delay does not affect the goodness of the estimate of total deaths: the model predicts 1,201 fatalities versus 1,166 officially registered.

From Fig. 4, right panel, it can be seen how the model simulates the *speed* of the Nigerian vaccination campaign with an initial steep slope followed by a progressively decline in the final stage of the outbreak.

According to model (6), the vaccination campaign was able to reduce the reproduction number but not below the threshold $\mathcal{R}_V = 1$. In fact, in view of (9), (10) and Table 1, the basic reproduction number is $\mathcal{R}_0 \approx 1.89$, while the control reproduction number is $\mathcal{R}_V \approx 1.66$. Now, when $\mathcal{R}_V > 1$ we know from Proposition 5 that the model may admit one or three endemic equilibria. However, when the parameter values in Table 1 are considered, we have an unique (and stable) endemic equilibrium EE since the polynomial (14) has all real roots and $b_0 < 0$, $b_i > 0$, $i = 1, \ldots, 3$, as it can be verified by direct computation. The components of EE are given in (13), where λ_e is the unique positive real root of (14). In particular, from the expression of the endemic number of ill cases, I_e, we can deduce that this value reduces from about 221 individuals in absence of vaccination to 190 individuals when vaccination is in place.

Model (6) may be used to estimate the unreported data. In Fig. 5 it is shown the time evolution of susceptibles and carriers, and the prevalence of ill cases. We note that the number of asymptomatic carriers predicted by the model is much higher than the number of ill cases. The predicted peak of carriers is around 25.5 $\cdot 10^6$ individuals (i.e. 13.7% of the total population). This appears to be in agreement with several studies about meningococcal carriage in the African meningitis belt, according to which carriage prevalences range from 3% to 30% (see [46] and references therein).

Besides of the comparison with the official data, the model may be also used to simulate the outcome produced by hypothetical strategies of containment enacted by the health authorities. According to WHO, vaccination campaigns against meningitis outbreaks

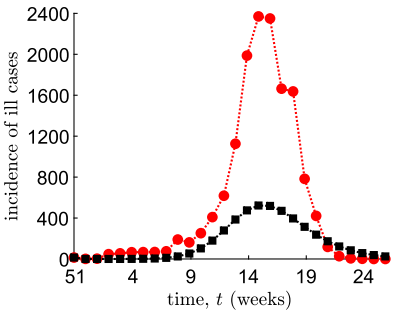

Fig. 6. Weekly incidence of ill cases. Comparison between the official data of 2016/2017 Nigerian outbreak (red dots) and the solutions of model (6) (black line) in the case of the Highest Level of Intervention. The ticks on the horizontal axis correspond to the first day of the indicated epidemiological week. Initial conditions and parameter values are given in Table 1 or otherwise specified in Section 6.

should be conducted within four weeks of crossing the epidemic threshold [47]. In the case of the Nigerian outbreak under consideration, the first LGA that passed the epidemic threshold was Birnin Magaji in the epidemiological week 3 of 2017 [39]. This means that, according to WHO, the vaccination campaign should have started at most in the epidemiological week 7 of 2017 instead of the week 14. Therefore, it can be of interest to assess the impact on the epidemic course of a vaccination campaign starting on the recommended deadline (i.e. February 13, the beginning of epidemiological week 7) and implemented at the maximum possible rate. We will refer to this case as the Highest Level of Intervention (HLI).

According to model (6), the maximum possible vaccination rate is obtained when $p_0 + p_1(M) = p_{\max}$, where $p_{\max}$ is given in Table 1. To realize this condition, we consider the case of fully mandatory vaccination ($p_0 = p_{\max}$, $p_1(M) = 0$), although the maximum vaccination rate may also result from very high reactivity of individuals to voluntary vaccination ($D \to +\infty$). Under the HLI scenario, numerical simulations make it possible to estimate that almost 64% of the total Nigerian population would have been vaccinated, i.e. almost all the people aged 1–29 years. Moreover, in spite of the success of the vaccination campaign, the incidence of ill cases would have been still significant, especially in the weeks around the peak (see Fig. 6). Cumulatively, the total number of ill cases and deaths would have been 4,838 and 390, respectively (about 67% less than the registered ones).

7. Conclusions

Our study concerns with a behavioural vaccination model with application to a real case of meningitis outbreak in Nigeria. From the point of view of meningitis disease modelling, there is a large literature where the disease transmission and its control are investigated. However, there is only one previous work which makes use of the information index to take into account the social aspects of a vaccination campaign for meningitis [21]. Our study improves what done in [21] since we consider the more realistic case of an imperfect vaccine and the theoretical qualitative analysis is combined with an application based on official data regarding a real meningitis epidemic. From the point of view of behavioural modelling of infectious diseases, so far the only application to a real case of models including an information index is limited to a COVID–19 specific case [24]. Therefore, this application to the meningitis case shows the broad potential use of this modelling approach.

Firstly, we perform a qualitative analysis of the model based on stability and bifurcation theories, and obtain the following results:

i) voluntary vaccination is unable to eliminate the disease, since the control reproduction number $\mathcal{R}_V$ is independent of information parameters;
ii) a partially or fully mandatory vaccination always leads to $\mathcal{R}_V < \mathcal{R}_0$, although the vaccine is imperfect (see the inequality (11));
iii) the model may admit multiple endemic equilibria both below and above the critical threshold $\mathcal{R}_V = 1$. This is consistent with the dynamics observed for SIS–like behavioural models with imperfect vaccination [48,49].

Secondly, the model is parametrized by using official data regarding the largest ever global epidemic of serogroup C meningitis occurred in Nigeria from December 2016 to June 2017. We provide numerical investigations focusing on both the *uncontrolled* phase of the epidemic and the *controlled* phase, where a vaccination campaign is implemented. We find that:

i) two fundamental information–related quantities can be estimated: k, the information coverage regarding the number of ill cases (normalized with respect to $\bar{N}$) and $1/a$, the information delay. We find $k = 0.69$, meaning that the public was aware of about 69% of official data, and $1/a = 4.27$ days, the average time lag necessary for information to reach the public;
ii) the model provides estimates of the unreported data, like the epidemic evolution of susceptibles, carriers and the prevalence of ill cases. In particular, the model indicates a peak of asymptomatic carriers around 13.7% of the total population. This is in agreement with studies on meningococcal carriage in the African meningitis belt [46];
iii) the model estimates that the incidence of ill cases would have been still significant, especially during the weeks around the peak, even in the hypothetical case of an early and massive vaccination campaign. Cumulatively, both the total number of ill cases and the total deaths would have been about 67% less than the registered ones.

Shaping the complex interaction between circulating information, human behaviour and epidemic disease is very challenging, and several open problems need to be addressed.

Our work has of course some limitations. A first issue is that field data about vaccinating attitudes are unknown, so that we use a Holling type II function to qualitatively represent the information–dependent vaccination rate. However, it is necessary to explore different functional responses to alternatively describe the reactivity of individuals and to assess which functional response gives the best match with official data.

Another main limitation is that we consider a single homogeneous age group, since children and young adults – the individuals at highest risk of meningitis [1] – constitute most of the population in sub–Saharan Africa [50]. However, when different diseases and/or different geographic areas are considered, it might be needed to explicitly include the age structure in the model.

These limitations offer opportunities of future directions. Another potential extension of our study is the inclusion of seasonal patterns that are not considered here, since the model describes a single meningitis outbreak occurred during the dry season. It is well known that seasonality may induce complex dynamics in epidemic models and is often the primary factor responsible for recurrent epidemic waves [51]. On one hand, meningitis models with seasonality have already been considered in some studies [4,5]. On the other hand, the interplay between behavioural responses and seasonality is a major topic of the mathematical modelling of infectious diseases [52]. Therefore, it would be of interest to study such interplay in the perspective of meningitis disease.

Finally, some authors used meningitis models to investigate the optimal strategy for curtailing the spread of the disease. The control variables may represent personal protection such as the use of vaccination and facial masks [11,16]. These problems are usually studied by using an optimal control approach based on the Pontryagin Maximum Principle. Currently, there is a substantial lack of papers coupling information index and optimal control. However, it has been shown that the optimal control of social distancing is able to generate interesting period doubling–like phenomena when the disease transmission is described by behavioural SIR models with information index [53]. Control problems related to more complex models like the one considered here are a challenging future perspective.

Declaration of competing interest

The authors declare that they have no known competing financial interests or personal relationships that could have appeared to influence the work reported in this paper.

Data availability

Data will be made available on request.

Acknowledgements

We thank the editors and the reviewers for their careful reading and their useful comments. This work has been performed under the auspices of the Italian National Group for Mathematical Physics (GNFM) of the National Institute for Advanced Mathematics (INdAM).

This research was supported by EU funding within the NextGenerationEU—MUR PNRR Extended Partnership initiative on Emerging Infectious Diseases (Project no. PE00000007, INF-ACT).

B.B. also acknowledges PRIN 2020 project (No. 2020JLWP23) “Integrated Mathematical Approaches to Socio–Epidemiological Dynamics”.

Appendix A

A.1. Positively invariant region

By standard procedure (see e.g. [54]), from (6)–(7) one can derive that

$$S > 0,\ V \geq 0,\ C \geq 0,\ I \geq 0,\ R \geq 0,\ M \geq 0,$$

for all $t \geq 0$.

Adding the first five equations of system (6), one gets

$$\dot{N} = \Lambda - \mu N - d I, \tag{22}$$

and taking into account that $0 \leq I \leq N$, it follows that $\dot{N} \leq \Lambda - \mu N$. If $N(0) \leq \Lambda/\mu$, then for all $t \geq 0$

$$N(t) \leq N(0)e^{-\mu t} + \frac{\Lambda}{\mu}\left(1 - e^{-\mu t}\right) \leq \frac{\Lambda}{\mu}.$$

Finally, from the definition of M given in (3) and $I \leq \Lambda/\mu$, it easily follows that $M \leq k$ for all $t \geq 0$.

A.2. Derivation of the reproduction numbers

Following the procedure and the notations adopted by Diekmann *et al.* [55] and Van den Driessche and Watmough [29], we first derive the control reproduction number, $\mathcal{R}_V$.

Let us consider the balance equations of the infected compartments (6c)–(6d) and define the vector $\mathcal{F}_0$ of the transmission terms contained therein, that is

$$\mathcal{F}_0 = \begin{pmatrix} \beta(S+(1-\psi)V)\dfrac{\varepsilon C+I}{N} \\ 0 \end{pmatrix},$$

and the vector $\mathcal{F}_1$ of all the other rates of transfer, that is

$$\mathcal{F}_1 = \begin{pmatrix} (\sigma+\delta+\mu)C \\ -\sigma C+(\rho+\mu+d)I \end{pmatrix}.$$

The procedure in [29,55] requires to compute the Jacobian matrices of $\mathcal{F}_0$ and $\mathcal{F}_1$ evaluated at the DFE (8). In our case, these are

$$\mathrm{F}_0 = \begin{pmatrix} \beta\varepsilon\dfrac{(1-\psi)p_0+\theta+\mu}{p_0+\theta+\mu} & \beta\dfrac{(1-\psi)p_0+\theta+\mu}{p_0+\theta+\mu} \\ 0 & 0 \end{pmatrix}, \tag{23}$$

and

$$\mathrm{F}_1 = \begin{pmatrix} \sigma+\delta+\mu & 0 \\ -\sigma & \rho+\mu+d \end{pmatrix}, \tag{24}$$

respectively. As proved in [29,55], the control reproduction number is given by the spectral radius of the *next generation* matrix $\mathrm{F}_0\mathrm{F}_1^{-1}$. It is easy to check that in our case $\mathcal{R}_V$ is given by the first diagonal element of $\mathrm{F}_0\mathrm{F}_1^{-1}$, that is

$$\mathcal{R}_V = (\mathrm{F}_0\mathrm{F}_1^{-1})_{11} = \beta\frac{(1-\psi)p_0+\theta+\mu}{p_0+\theta+\mu}\,\frac{\varepsilon(\rho+\mu+d)+\sigma}{(\sigma+\delta+\mu)(\rho+\mu+d)}.$$

Without vaccination one has $p_0 = 0$ and the basic reproduction number is given in (9). More formally, when vaccination is not considered, system (6) reduces to

$$\begin{aligned} \dot{S} &= \Lambda-\beta S\frac{\varepsilon C+I}{N}+\phi R-\mu S, \\ \dot{C} &= \beta S\frac{\varepsilon C+I}{N}-(\sigma+\delta+\mu)C, \\ \dot{I} &= \sigma C-(\rho+\mu+d)I, \\ \dot{R} &= \delta C+\rho I-(\phi+\mu)R. \end{aligned} \tag{25}$$

The expression of $\mathcal{R}_0$ may be obtained by repeating the same procedure for system (25).

A.3. Global stability of the DFE

We adopt the approach developed by Kamgang and Sallet [56]. System (6) may be rewritten in the form

$$\begin{aligned} \dot{x}_1 &= A_1(x)(x_1-x_1^0)+A_{12}(x)x_2, \\ \dot{x}_2 &= A_2(x)x_2, \end{aligned} \tag{26}$$

where $x=(x_1,x_2)$, being $x_1=(S,V,R,M)^T$ and $x_2=(C,I)^T$ the vectors of uninfected and infected compartments, respectively. Using such notations, the DFE may be written as $(x_1^0,0,0)^T$, where $x_1^0=(\bar{S},\bar{V},0,0)$. One can easily verify that

$$A_1 = \begin{pmatrix} -(p_0+\mu) & \theta & \phi & -(p_{\max}-p_0)\dfrac{DS}{1+DM} \\ p_0 & -(\theta+\mu) & 0 & (p_{\max}-p_0)\dfrac{DS}{1+DM} \\ 0 & 0 & -(\phi+\mu) & 0 \\ 0 & 0 & 0 & -a \end{pmatrix},$$

$$A_{12} = \begin{pmatrix} -\dfrac{\beta\varepsilon}{N}S & -\dfrac{\beta}{N}S \\ -(1-\psi)\dfrac{\beta\varepsilon}{N}V & -(1-\psi)\dfrac{\beta}{N}V \\ \delta & \rho \\ 0 & ah \end{pmatrix},$$

and

$$A_2 = \begin{pmatrix} \frac{\beta\varepsilon}{N}(S+(1-\psi)V) - (\sigma+\delta+\mu) & \frac{\beta}{N}(S+(1-\psi)V) \\ \sigma & -(\rho+\mu+d) \end{pmatrix}. \tag{27}$$

Then, the DFE is globally asymptotically stable, provided that the following conditions are satisfied (see [56], Theorem 4.3):

C1. The system (26) is defined on a positively invariant region Ω of the nonnegative orthant, and is dissipative on Ω.
C2. The equilibrium x_1^0 is globally asymptotically stable for the sub–system $\dot{x}_1 = A_1(x_1, 0)(x_1 - x_1^0)$.
C3. The matrix A_2 is Metzler (i.e., the off–diagonal elements are nonnegative) and irreducible.
C4. There exists an upper bound matrix $\tilde{A}_2$ for $\mathcal{M} = \{A_2(x), x \in \Omega\}$ with the property that either $\tilde{A}_2 \notin \mathcal{M}$ or if $\tilde{A}_2 \in \mathcal{M}$ (i.e., $\tilde{A}_2 = \max_\Omega \mathcal{M}$), then for any $\tilde{x} = (\tilde{x}_1, \tilde{x}_2) \in \Omega$ such that $\tilde{A}_2 = A_2(\tilde{x})$, it follows that $\tilde{x}_2 = 0$ (i.e., the points where the maximum is realized are contained in the disease–free sub–manifold).
C5. The stability modulus (i.e., the greatest real part of the eigenvalues) of $\tilde{A}_2$ is nonpositive.

Condition C1 is a direct consequence of Proposition 1.

The sub–system mentioned in Condition C2 is

$$\begin{aligned} \dot{S} &= \Lambda - \left(p_0 + (p_{\max} - p_0)\frac{DM}{1+DM}\right)S + \theta V + \phi R - \mu S, \\ \dot{V} &= \left(p_0 + (p_{\max} - p_0)\frac{DM}{1+DM}\right)S - (\theta+\mu)V, \\ \dot{R} &= -(\phi+\mu)R, \\ \dot{M} &= -aM, \end{aligned}$$

so that

$$(S, V, R, M) \to \left(\frac{\Lambda(\theta+\mu)}{\mu(p_0+\theta+\mu)}, \frac{\Lambda p_0}{\mu(p_0+\theta+\mu)}, 0, 0\right), \text{ as } t \to +\infty.$$

Therefore, Condition C2 is also verified.

From (27) we note that the matrix A_2 is Metzler. Moreover, being the off–diagonal elements of A_2 nonnull, the graph associated to A_2 is strongly connected, that is A_2 is irreducible [57]. Hence, Condition C3 is satisfied.

The matrix $\tilde{A}_2$ required by Condition C4 is

$$\tilde{A}_2 = \begin{pmatrix} \beta\varepsilon - (\sigma+\delta+\mu) & \beta \\ \sigma & -(\rho+\mu+d) \end{pmatrix},$$

since $S + (1-\psi)V \le S + V \le N$ in Ω, and $\tilde{A}_2 \in \mathcal{M}$ only if $S = N$ and $V = C = I = R = 0$, so that $\tilde{x}_2 = 0$.

Finally, all the eigenvalues of $\tilde{A}_2$ have nonpositive real part if, and only if, $\det(\tilde{A}_2) \ge 0$ and $\mathrm{tr}(\tilde{A}_2) \le 0$, which is equivalent to

$$\beta(\varepsilon(\rho+\mu+d)+\sigma) \le (\sigma+\delta+\mu)(\rho+\mu+d),$$

i.e. to the hypothesis $\mathcal{R}_0 \le 1$. Therefore, Condition C5 is also satisfied.

References

[1] World Health Organization, Meningitis, https://www.who.int/news-room/fact-sheets/detail/meningitis. (Accessed February 2023), 2023.
[2] World Health Organization, Meningococcal meningitis, https://www.who.int/teams/health-product-policy-and-standards/standards-and-specifications/vaccine-standardization/meningococcal-meningitis. (Accessed February 2023), 2023.
[3] N.E. Basta, A. Berthe, M. Keita, U. Onwuchekwa, B. Tamboura, A. Traore, M. Hassan-King, O. Manigart, M. Nascimento, J.M. Stuart, C. Trotter, J. Blake, A.D. Carr, S.J. Gray, L.S. Newbold, Y. Deng, J. Wolfson, M.E. Halloran, B. Greenwood, R. Borrow, S.O. Sow, Meningococcal carriage within households in the African meningitis belt: a longitudinal pilot study, J. Infect. 76 (2) (2018) 140–148, https://doi.org/10.1016/j.jinf.2017.11.006.
[4] T.J. Irving, K.B. Blyuss, C. Colijn, C.L. Trotter, Modelling meningococcal meningitis in the African meningitis belt, Epidemiol. Infect. 140 (5) (2012) 897–905, https://doi.org/10.1017/S0950268811001385.
[5] T. Koutangni, P. Crépey, M. Woringer, S. Porgho, B.W. Bicaba, H. Tall, J.E. Mueller, Compartmental models for seasonal hyperendemic bacterial meningitis in the African meningitis belt, Epidemiol. Infect. 147 (2019) e14, https://doi.org/10.1017/S0950268818002625.
[6] Centers for Disease Control and Prevention, Meningococcal disease, https://www.cdc.gov/meningococcal/index.html. (Accessed March 2023), 2023.
[7] P.C. McCarthy, A. Sharyan, L. Sheikhi Moghaddam, Meningococcal vaccines: current status and emerging strategies, Vaccines 6 (1) (2018) 12, https://doi.org/10.3390/vaccines6010012.
[8] F.M. LaForce, M. Djingarey, S. Viviani, M.P. Preziosi, Successful African introduction of a new group A meningococcal conjugate vaccine: future challenges and next steps, Human Vaccines Immunother. 14 (5) (2018) 1098–1102, https://doi.org/10.1080/21645515.2017.1378841.
[9] J.E. Mueller, Long–term effectiveness of MenAfriVac, Lancet Infect. Dis. 19 (3) (2019) 228–229, https://doi.org/10.1016/S1473-3099(18)30725-4.
[10] M. White, O. Idoko, S. Sow, A. Diallo, B. Kampmann, R. Borrow, C. Trotter, Antibody kinetics following vaccination with MenAfriVac: an analysis of serological data from randomised trials, Lancet Infect. Dis. 19 (3) (2019) 327–336, https://doi.org/10.1016/S1473-3099(18)30674-1.
[11] F. Agusto, M. Leite, Optimal control and cost–effective analysis of the 2017 meningitis outbreak in Nigeria, Infect. Dis. Model. 4 (2019) 161–187, https://doi.org/10.1016/j.idm.2019.05.003.
[12] G. Djatcha Yaleu, S. Bowong, E.H. Danga, J. Kurths, Mathematical analysis of the dynamical transmission of Neisseria meningitidis serogroup A, Int. J. Comput. Math. 94 (12) (2017) 2409–2434, https://doi.org/10.1080/00207160.2017.1283411.
[13] J.L. Simpson, M.G. Roberts, Modelling the effect of vaccination on the meningococcal B epidemic in New Zealand, ANZIAM J. 54 (1–2) (2012) 74–88, https://doi.org/10.1017/S1446181113000047.

[14] C.L. Trotter, N.J. Gay, W.J. Edmunds, Dynamic models of meningococcal carriage, disease, and the impact of serogroup C conjugate vaccination, Am. J. Epidemiol. 162 (1) (2005) 89–100, https://doi.org/10.1093/aje/kwi160.
[15] H.C. Tuckwell, T. Hanslik, A.J. Valleron, A. Flahault, A mathematical model for evaluating the impact of vaccination schedules: application to Neisseria meningitidis, Epidemiol. Infect. 130 (3) (2003) 419–429, https://doi.org/10.1017/S0950268803008501.
[16] J.K.K. Asamoah, F. Nyabadza, Z. Jin, E. Bonyah, M.A. Khan, M.Y. Li, T. Hayat, Backward bifurcation and sensitivity analysis for bacterial meningitis transmission dynamics with a nonlinear recovery rate, Chaos Solitons Fractals 140 (2020) 110237, https://doi.org/10.1016/j.chaos.2020.110237.
[17] S. Collinson, K. Khan, J.M. Heffernan, The effects of media reports on disease spread and important public health measurements, PLoS ONE 10 (11) (2015) 1–21, https://doi.org/10.1371/journal.pone.0141423.
[18] Z. Wang, C.T. Bauch, S. Bhattacharyya, A. d'Onofrio, P. Manfredi, M. Perc, N. Perra, M. Salathé, D. Zhao, Statistical physics of vaccination, Phys. Rep. 664 (2016) 1–113, https://doi.org/10.1016/j.physrep.2016.10.006.
[19] S. Cooper, C. Betsch, E.Z. Sambala, N. Mchiza, C.S. Wiysonge, Vaccine hesitancy – a potential threat to the achievements of vaccination programmes in Africa, Human Vaccines Immunother. 14 (10) (2018) 2355–2357, https://doi.org/10.1080/21645515.2018.1460987.
[20] European Centre for Disease Prevention and Control, Catalogue of interventions addressing vaccine hesitancy, https://www.ecdc.europa.eu/en/publications-data/catalogue-interventions-addressing-vaccine-hesitancy. (Accessed April 2023), 2017.
[21] B. Buonomo, A. d'Onofrio, S.M. Kassa, Y.H. Workineh, Modeling the effects of information-dependent vaccination behavior on meningitis transmission, Math. Methods Appl. Sci. 45 (2) (2022) 732–748, https://doi.org/10.1002/mma.7808.
[22] P. Manfredi, A. d'Onofrio (Eds.), Modeling the Interplay Between Human Behavior and the Spread of Infectious Diseases, Springer, New York, 2013.
[23] Nigeria Centre for Disease Control and Prevention, An update of meningitis outbreak in Nigeria, https://www.ncdc.gov.ng/diseases/sitreps/?cat=6&name=An%20Update%20of%20Meningitis%20Outbreak%20in%20Nigeria. (Accessed April 2023), 2022.
[24] B. Buonomo, R. Della Marca, Effects of information–induced behavioural changes during the COVID–19 lockdowns: the case of Italy, R. Soc. Open Sci. 7 (10) (2020) 201635, https://doi.org/10.1098/rsos.201635.
[25] B. Buonomo, R. Della Marca, A. d'Onofrio, M. Groppi, A behavioural modelling approach to assess the impact of COVID–19 vaccine hesitancy, J. Theor. Biol. 534 (2022) 110973, https://doi.org/10.1016/j.jtbi.2021.110973.
[26] A. d'Onofrio, P. Manfredi, E. Salinelli, Vaccinating behaviour, information, and the dynamics of SIR vaccine preventable diseases, Theor. Popul. Biol. 71 (3) (2007) 301–317, https://doi.org/10.1016/j.tpb.2007.01.001.
[27] B. Buonomo, A. d'Onofrio, D. Lacitignola, Global stability of an SIR epidemic model with information dependent vaccination, Math. Biosci. 216 (1) (2008) 9–16, https://doi.org/10.1016/j.mbs.2008.07.011.
[28] N. MacDonald, Biological Delay Systems: Linear Stability Theory, Cambridge University Press, Cambridge, 1989.
[29] P. Van den Driessche, J. Watmough, Reproduction numbers and sub–threshold endemic equilibria for compartmental models of disease transmission, Math. Biosci. 180 (1) (2002) 29–48, https://doi.org/10.1016/S0025-5564(02)00108-6.
[30] C. Castillo-Chavez, B. Song, Dynamical models of tuberculosis and their applications, Math. Biosci. Eng. 1 (2) (2004) 361–404, https://doi.org/10.3934/mbe.2004.1.361.
[31] J. Dushoff, W. Huang, C. Castillo-Chavez, Backwards bifurcations and catastrophe in simple models of fatal diseases, J. Math. Biol. 36 (3) (1998) 227–248, https://doi.org/10.1007/s002850050099.
[32] J. Guckenheimer, P. Holmes, Nonlinear Oscillations, Dynamical Systems, and Bifurcations of Vector Fields, Springer, Berlin, 1983.
[33] National Bureau of Statistics, Demographic statistics bulletin, Nigeria, https://tinyurl.com/2tmw7e63. (Accessed April 2023), 2020.
[34] The World Bank, Life expectancy at birth, total (years) – Nigeria, https://data.worldbank.org/indicator/SP.DYN.LE00.IN?locations=NG. (Accessed April 2023), 2022.
[35] K.R. Fister, H. Gaff, S. Lenhart, E. Numfor, E. Schaefer, J. Wang, Optimal control of vaccination in an age–structured cholera model, in: G. Chowell, J.M. Hyman (Eds.), Mathematical and Statistical Modeling for Emerging and Re-Emerging Infectious Diseases, Springer, Cham, 2016, pp. 221–248.
[36] S. Lee, M. Golinski, G. Chowell, Modeling optimal age–specific vaccination strategies against pandemic influenza, Bull. Math. Biol. 74 (4) (2012) 958–980, https://doi.org/10.1007/s11538-011-9704-y.
[37] E. Shim, Optimal dengue vaccination strategies of seropositive individuals, Math. Biosci. Eng. 16 (3) (2019) 1171–1189, https://doi.org/10.3934/mbe.2019056.
[38] L.V. Cooper, O. Ronveaux, K. Fernandez, C. Lingani, K. Goumbi, C. Ihekweazu, M.P. Preziosi, A. Durupt, C.L. Trotter, Spatiotemporal analysis of serogroup C meningococcal meningitis spread in Niger and Nigeria and implications for epidemic response, J. Infect. Dis. 220 (Suppl. 4) (2019) S244–S252, https://doi.org/10.1093/infdis/jiz343.
[39] A. Hassan, G.U. Mustapha, B.B. Lawal, A.M. Na'uzo, R. Ismail, E. Womi-Eteng Oboma, O. Oyebanji, J. Agenyi, C. Thomas, M.S. Balogun, M.M. Dalhat, P. Nguku, C. Ihekweazu, Time delays in the response to the Neisseria meningitidis serogroup C outbreak in Nigeria – 2017, PLoS ONE 13 (6) (2018) 1–13, https://doi.org/10.1371/journal.pone.0199257.
[40] C. Nnadi, J. Oladejo, S. Yennan, A. Ogunleye, C. Agbai, L. Bakare, M. Abdulaziz, A. Mohammed, M. Stephens, K. Sumaili, O. Ronveaux, H. Maguire, D. Karch, M. Dalhat, M. Antonio, A. Bita, I. Okudo, P. Nguku, R. Novak, O. Bolu, F. Shuaib, C. Ihekweazu, Large outbreak of Neisseria meningitidis Serogroup C – Nigeria, December 2016–June 2017, Morb. Mort. Wkly. Rep. 66 (49) (2017) 1352–1356, https://doi.org/10.15585/mmwr.mm6649a3.
[41] World Health Organization Africa, End of meningitis outbreak in Nigeria, December 2016–June 2017, https://www.afro.who.int/sites/default/files/2017-09/Dashboard%20of%20Nigeria%20meningitis%20-%20EndF.pdf. (Accessed March 2023), 2017.
[42] Princeton University – Emergency Management, Meningitis FAQ – General Information, https://emergency.princeton.edu/FAQMeningitisB. (Accessed March 2023), 2019.
[43] T. Day, On the evolution of virulence and the relationship between various measures of mortality, Proc. R. Soc. Lond. B, Biol. Sci. 269 (1498) (2002) 1317–1323, https://doi.org/10.1098/rspb.2002.2021.
[44] A.B. Gumel, S. Ruan, T. Day, J. Watmough, F. Brauer, P. Van den Driessche, D. Gabrielson, C. Bowman, M.E. Alexander, S. Ardal, J. Wu, B.M. Sahai, Modelling strategies for controlling SARS outbreaks, Proc. R. Soc. Lond. B, Biol. Sci. 271 (1554) (2004) 2223–2232, https://doi.org/10.1098/rspb.2004.2800.
[45] MATLAB, Matlab Release 2023a, The MathWorks, Inc., Natick, MA, 2023.
[46] C.L. Trotter, B.M. Greenwood, Meningococcal carriage in the African meningitis belt, Lancet Infect. Dis. 7 (12) (2007) 797–803, https://doi.org/10.1016/S1473-3099(07)70288-8.
[47] World Health Organization, Meningitis outbreak response in sub–Saharan Africa: WHO guideline, http://apps.who.int/iris/handle/10665/144727. (Accessed April 2023), 2014.
[48] B. Buonomo, R. Della Marca, Oscillations and hysteresis in an epidemic model with information–dependent imperfect vaccination, Math. Comput. Simul. 162 (2019) 97–114, https://doi.org/10.1016/j.matcom.2019.01.005.
[49] A. d'Onofrio, P. Manfredi, Bistable endemic states in a susceptible–infectious–susceptible model with behavior–dependent vaccination, in: G. Chowell, J. Hyman (Eds.), Mathematical and Statistical Modeling for Emerging and Re–emerging Infectious Diseases, Springer, Cham, 2016, pp. 341–354.
[50] United Nations, Population division – world population prospects 2022, https://population.un.org/wpp/Graphs/Probabilistic/PopPerc/1834. (Accessed March 2023), 2022.
[51] R. Olinky, A. Huppert, L. Stone, Seasonal dynamics and thresholds governing recurrent epidemics, J. Math. Biol. 56 (2008) 827–839, https://doi.org/10.1007/s00285-007-0140-4.
[52] A. d'Onofrio, P. Manfredi, Behavioral SIR models with incidence–based social-distancing, Chaos Solitons Fractals 159 (2022) 112072, https://doi.org/10.1016/j.chaos.2022.112072.

[53] S.S. Sharbayta, B. Buonomo, A. d'Onofrio, T. Abdi, 'Period doubling' induced by optimal control in a behavioral SIR epidemic model, Chaos Solitons Fractals 161 (2022) 112347, https://doi.org/10.1016/j.chaos.2022.112347.
[54] S. Sharma, G.P. Samanta, Analysis of a drinking epidemic model, Int. J. Dyn. Control 3 (3) (2015) 288–305, https://doi.org/10.1007/s40435-015-0151-8.
[55] O. Diekmann, J.A.P. Heesterbeek, J.A.J. Metz, On the definition and the computation of the basic reproduction ratio R_0 in models for infectious diseases in heterogeneous populations, J. Math. Biol. 28 (4) (1990) 365–382, https://doi.org/10.1007/BF00178324.
[56] J.C. Kamgang, G. Sallet, Computation of threshold conditions for epidemiological models and global stability of the disease-free equilibrium (DFE), Math. Biosci. 213 (1) (2008) 1–12, https://doi.org/10.1016/j.mbs.2008.02.005.
[57] H. Guo, M.Y. Li, Z. Shuai, Global stability of the endemic equilibrium of multigroup SIR epidemic models, Can. Appl. Math. Q. 14 (3) (2006) 259–284, https://doi.org/10.1016/j.camwa.2010.08.020.